

Microemulsions Improve Topical Protoporphyrin IX (PpIX) Delivery for Photodynamic Therapy of Skin Cancer

Paula Ângela de Souza Marinho Leite¹, Nadia Campos de Oliveira Miguel²,
Maria Bernadete Riemma Pierre^{1*}

¹Faculdade de Farmácia, Universidade Federal do Rio de Janeiro, RJ, Brazil, ²Instituto de Ciências Biomédicas, Universidade Federal do Rio de Janeiro, Rio de Janeiro, RJ, Brazil

We report here microemulsions (MEs) for topical delivery of protoporphyrin IX (PpIX) for Photodynamic Therapy (PDT) of skin cancers. Selected MEs consisting of Oil/Water (O/W) bicontinuous (BC) and Water/Oil (W/O) preparations were characterized as to pH, nanometric size, zeta potential, drug content, and viscosity. Sustained *in vitro* PpIX release was achieved from MEs 2A (O/W), 10B (BC) and 16B (W/O) through an artificial membrane for up to 24 h, characterizing MEs as drug delivery systems. None of these MEs showed permeation through the skin, demonstrating the required topical effect. After 4 h, *in vitro* retention of PpIX in the *stratum corneum* (SC) was higher from both ME 10B and control (PpIX at 60 µg/mL in PEG 300). However, in the Epidermis + Dermis ([Ep + D]), retention from ME 10B and ME 16B was ~40 times higher compared to control. Confocal Laser Scanning Microscopy (CLSM) showed higher fluorescence intensity in the SC for both control and ME 10B, whereas ME 10B fluorescence was higher in [Ep+D]. The results indicate that ME 10B is suitable for PpIX encapsulation, showing good characteristics and a localized effect for a potential delivery system for PDT-associated treatments of skin cancers.

Keywords: Protoporphyrin IX. Photodynamic therapy. Skin cancer. Microemulsion. *In vitro* skin retention.

INTRODUCTION

Skin cancer accounts for 33% of all cancer diagnoses in Brazil, with approximately 180,000 new cases registered each year by the National Cancer Institute (INCA). Among non-melanoma skin cancers (NMSC), the most common types are basal cell carcinoma (BCC), the most prevalent one that appears in basal cells located in the deepest layer of the epidermis, and squamous cell carcinoma (SCC) which appears in squamous cells of the epidermis (Inca, 2022).

All cases of skin cancer must be diagnosed and treated early, including those of low lethality, which can cause

mutilating or disfiguring lesions in exposed areas of the body. Fortunately, there are several therapeutic options for the treatment of NMSC. Photodynamic Therapy (PDT) is a minimally invasive therapeutic modality used to treat various cancers and premalignant diseases (Wachowska *et al.*, 2011) which has shown efficacy for BCC, superficial SCC, and actinic keratosis (AK) with success rates above 80% (Dögnitz *et al.*, 2008). In this therapy, a photosensitizing agent (PS), light and oxygen cause selective tissue destruction. PS are light-absorbing species with adequate energy and/or electron transfer properties.

PDT has numerous advantages over conventional treatments for NMSC such as the low number of sessions and the simultaneous treatment of several lesions, a low rate of side effects, destruction of tumor vascularization, little or no scarring after healing, and the lowest cost. However, since oxygenation is crucial for the

*Correspondence: M. B. R. Pierre. Faculdade de Farmácia. Universidade Federal do Rio de Janeiro. Av. Carlos Chagas Filho, 373. 21.941.590, Rio de Janeiro, Brazil. Phone/fax: + 55 21 2260.91.92 branch 258. E-mail: bernadete@pharma.ufrj.br. ORCID: <https://orcid.org/0000-0002-7893-3172>

photodynamic effect, disseminated metastases, tumors surrounded by necrotic tissues and dense tumor masses are difficult to treat (Calixto *et al.*, 2016).

Two PS groups such as porphyrin-derived and non-porphyrin-based agents are currently available. Those approved for clinical use in PDT are Porphimer sodium (Photofrin[®]), 5-aminolevulinic acid (5-ALA, Levulan[®]) and its methyl ester MAL (Metvix[®]), temoporfin[®] (Foscan[®]), verteporfin (Visudyne[®]), and talaporfin (Laserphyrin[®]) (Wachowska *et al.*, 2011).

5-Aminoluvulinic acid (5-ALA) is a prodrug widely used in PDT, being converted *in situ* by the heme biosynthetic route into the effective PS protoporphyrin IX (PpIX). The use of 5-ALA in PDT has been highly efficient for the treatment of various superficial skin diseases. However, 5-ALA is a hydrophilic molecule that poorly penetrates the hydrophobic *stratum corneum* (SC), this being the principal barrier to effective absorption (Donnelly, McCarron, Woolfson, 2005). Therefore, recurrence in nodular lesions can occur since the integrity of the SC is intact, as in normal skin (McLoone *et al.*, 2004).

An alternative is the direct use of PS PpIX instead of the 5-ALA prodrug, with the advantage of non-dependence on the bioconversion of 5-ALA into the active compound (Kloek, Akkermans, Van Henegouwen, 1998). Also, the high lipophilicity of PpIX allows for a better ability to produce cytotoxic species and more effective cell death, thus improving PDT procedures (Bonnet, 1995). However, the low solubility of PpIX in aqueous media causes high aggregation of its monomeric species into dimers. These species reduce singlet oxygen generation (responsible for cell damage), thus also reducing the photodynamic effect (Basoglu, Bilgin, Demir, 2016).

Nanotechnology strategies have been used in recent years to improve the efficiency of PDT. Chemotherapeutics incorporated into nanocarriers have shown better efficacy in both *in vitro* and *in vivo* studies (Deda, Araki, 2015; Qidwai *et al.*, 2020). Our research group has shown that polymeric nanoparticles (NPs) and nanodispersions of liquid-crystalline phases (NLPs) are potential delivery systems for topical PpIX application in PDT. NPs showed advantages such as greater localization of PpIX in the

deeper layers of animal model skin and did not cause damage to L929 fibroblast cells grown in the dark (without PDT), revealing good biocompatibility with healthy cells. In these cells, NP showed low phototoxicity in the presence of light (with PDT) with 100% cell recovery after PDT, indicating that NP-encapsulated PpIX are protected from photoactivation, an effect which is desirable in healthy cells (de Oliveira Miguel *et al.*, 2020). In another study, NPs were tested *in vitro* against skin melanoma cells (B16F10), resulting in maintenance of the photophysical properties of encapsulated PpIX and excellent phototoxicity, in addition to safe PDT due to the low cytotoxicity of PpIX in the dark (da Silva *et al.*, 2021). Nanodispersions increased the retention of PpIX in the skin both *in vitro* and *in vivo*, without causing irritation after application (Rossetti *et al.*, 2016).

Other nanostructured systems such as nanoemulsions (NE) and microemulsions (ME) offer considerable opportunity for topical drug delivery (Nastiti *et al.*, 2017). Because they have a small diameter and contain a high percentage of surfactant, MEs have excellent penetration rates in the deep layers of the stratum corneum (SC) compared to conventional formulations (Silva *et al.*, 2010).

In addition, they can target drugs to specific cells in the body and solubilize insoluble drugs (Damasceno *et al.*, 2011). Thus, MEs can represent an alternative for carrying PpIX in skin tissue, increasing its aqueous solubility and consequently reducing its aggregation without losing its photodynamic effect. Furthermore, the modulation of the high lipophilicity of PpIX by encapsulation can improve its skin penetration (De Campos Araújo, Thomazine, Lopez, 2010). This is important in the case of nodular tumors (which contain a thick SC layer) that hinder the absorption of PS into the tissue.

The objective of the present study was to develop and characterize MEs containing highly lipophilic PS (PpIX) regarding pH, size, zeta potential, centrifugation, electrical conductivity, and viscosity. *In vitro* release and cutaneous permeability of PpIX from MEs were determined using an artificial membrane and pig ear skin, respectively. The penetration depth of PpIX in porcine skin was evaluated by Confocal Laser Scanning Microscopy (CLSM).

MATERIAL AND METHODS

Chemicals

PpIX ($C_{34}H_{34}N_4O_4$, M.W: 562.7; ~95%), cetyl pyridinium chloride monohydrate (CPC), and Tween 80[®] were purchased from Sigma Aldrich (St. Louis, MO). Anhydrous dimethyl sulfoxide (DMSO) was obtained from Merck (Darmstadt, Germany). Polyethylene glycol 300 (PEG 300) was from Vetec (Duque de Caxias, Brazil). Sodium Phosphate Dibasic P.A. Anhydrous and Sodium Phosphate Monobasic P.A. Anhydrous, and a Fluoropore hydrophobic membrane in Polytetrafluoroethylene, 0.5 μ pores with 47 mm diameter (Millipore[®]) were purchased from VETEC, Brazil. All other reagents were of analytical grade and used without further purification.

Animals

Full- thickness skins from porcine ears used for *in vitro* permeation experiments were obtained from a local slaughterhouse right after the death of the animals. The dorsal skins of the ears were cleaned with distilled water and the muscle, adipose tissue, and subcutaneous tissues were removed with a scalpel. The skin samples were then wrapped with plastic film and aluminum foil and frozen at -20 °C until use (a maximum of 30 days) (Harrison, Barry, Dugard,1984).

Spectrofluorimetric assay conditions for PpIX quantification

PpIX was quantified in aqueous medium, named acceptor solution (AS), which consisted of 0.1 M phosphate buffer, pH 7.2, containing 45 mM cetyl pyridinium chloride (CPC). This medium can solubilize PpIX for *in vitro* cutaneous permeability and release studies. For the *in vitro* cutaneous retention studies using pig ear skin, PpIX was quantified with DMSO for the

extraction of PS from skin samples due to good solubility, as described by Rosseti *et al.*, 2010.

For both media, PpIX was quantified by spectrofluorimetric measurements with an Fp-6300 Spectrofluorometer Jasco (Tokyo, Japan) under conditions of excitation and emission wavelengths of $\lambda=400$ and $\lambda=632$ nm, respectively; bandwidth: 0.5 nm; excitation and emission slits: 10/10, in reference to a calibration curve of PpIX in aqueous medium or in DMSO (5–400 ng mL⁻¹, $r > 0.999$). All spectrofluorimetric measurements, ME preparation, characterization, and *in vitro* studies were performed under subdued light in order to prevent PpIX photobleaching.

Preparation and characterization of blank MEs (without PpIX)

Preparation

Different proportions of Tween 80 as Surfactant (S), Isopropyl Alcohol as Cosurfactant (Co-S), Oleic Acid (OA) as the oily phase, and distilled water as the aqueous phase were used in the MEs obtained (Table I).

MEs were prepared by the phase titration method: S and Co-S were mixed with a magnetic stirrer at 900 rpm for 60 minutes, with the mixture left to stand overnight. Next, OA was incorporated into the S + Co-S mixture with the aid of the Ultra-Turrax equipment for 2 minutes (4,200 rpm). The aqueous phase was added to complete 5 g, followed by stirring for 3 minutes at 4,200 rpm to form the ME.

Characterization

Blank MEs were chosen according to the Pseudo Ternary Phase Diagram, prepared with the SigmaPlot 14.0 software. Table II shows MEs subjected to the following analyses: pH, diameter, zeta potential, refractive index, and viscosity.

TABLE I - Percentages of the aqueous phase, oil phase and S+ Co-S for the MEs obtained: The total percentage of S+Co-S and the proportion of each are indicated

Name	Aqueous phase (%)	Oil phase (%)	$\Sigma S + Co-S$ (%)	S: Co-S
ME 1 (BC)	10	10	80	95 % :5 % 90 % :10 % 85 % :15 % 80 % :20 % 75 % :25 % (3:1) 66.6 % :33.3 % (2:1) 50 % :50 % (1:1) 40 % :60 % (2:3) 33.3 % :66.6 % (1:2) 25 % :75 % (1:3)
ME 2 (O/W)	20	10	70	90 % :10 % 85 % :15 % 80 % :20 % 75 % :25 % (3:1) 66.6 % :33.3 % (2:1) 60 % :40 % (3:2) 50 % :50 % (1:1) 40 % :60 % (2:3) 33.3 % :66.6 % (1:2) 25 % :75 % (1:3)
ME 9 (W/O)	10	20	70	95 % :5 % 90 % :10 % 85 % :15 % 80 % :20 % 75 % :25 % (3:1) 66.6 % :33.3 % (2:1) 60 % :40 % (3:2) 50 % :50 % (1:1) 40 % :60 % (2:3) 33.3 % :66.6 % (1:2) 25 % :75 % (1:3)

TABLE I - Percentages of the aqueous phase, oil phase and S+ Co-S for the MEs obtained: The total percentage of S+Co-S and the proportion of each are indicated

Name	Aqueous phase (%)	Oil phase (%)	$\Sigma S + Co-S$ (%)	S: Co-S
ME 10 (BC)	20	20	60	95 % :5 % 90 % :10 % 85 % :15 % 80 % :20 % 75 % :25 % (3:1) 66.6 % :33.3 % (2:1) 60 % :40 % (3:2) 50 % :50 % (1:1) 40 % :60 % (2:3) 33.3 % :66.6 % (1:2) 25 % :75 % (1:3)
ME 16 (W/O)	10	30	60	95 % :5 % 90 % :10 % 85 % :15 % 80 % :20 % 75 % :25 % (3:1) 66.6 % :33.3 % (2:1) 60 % :40 % (3:2) 50 % :50 % (1:1) 40 % :60 % (2:3) 33.3 % :66.6 % (1:2) 25 % :75 % (1:3)
ME 22 (W/O)	10	40	50	75 % :25 % (3:1) 33.3 % :66.6 % (1:2) 25 % :75 % (1:3)
ME 27 (W/O)	10	50	40	75 % :25 % (3:1)

Abbreviations: W/O: water in oil; O/W: oil in water and BC: bicontinuous

TABLE II - Blank MEs for characterization (pH, diameter/PDI, Zeta Potential (PZ), Refractive Index (RI), and Viscosity (cp) and the respective percentages of the aqueous phase, oil phase and total percentage of the S+ Co-S (the S:Co-S proportions are indicated in parenthesis).

<i>Formulations</i>	<i>Aqueous phase (%)</i>	<i>Oil phase (%)</i>	<i>S + Co-S % and (proportion)</i>
ME 2 (O/A)			
ME 2A			70 (3:1)
ME 2B			70 (2:1)
ME 2C	20	10	70 (1:1)
ME 2D			70 (1:2)
ME 2E			70 (1:3)
ME 10 (BC)			
ME 10 A			60 (3:1)
ME 10 B			60 (2:1)
ME 10 C	20	20	60 (1:1)
ME 10 D			60 (1:2)
ME 10 E			60 (1:3)
ME 16 (A/O)			
ME 16 A			60 (3:1)
ME 16 B			60 (2:1)
ME 16 C	10	30	60 (1:1)
ME 16 D			60 (1:2)
ME 16 E			60 (1:3)
ME 22 (A/O)			
ME 22 A	10	40	50 (1:2)
ME 22 B			50 (1:3)

pH measurements

pH (n=3) was measured at 25 °C with a PHS-3B potentiometer (PHTek, Brazil) previously calibrated with a buffer solution, pH 4.0 and 7.0.

Size/Polydispersity index (PDI) and Surface charge (zeta potential) determinations

Diameter/PDI as well as Zeta Potential (ZP) were measured by Dynamic Light Scattering using the nanosizer equipment Zetasizer Nano ZS (Malvern Instruments). For both measurements, formulations without PpIX were diluted in distilled water at a ratio of 1:200. Sample qualities were assessed by PDI calculated from the size and diameter data.

Refractive index

For accurate measurement of droplet size, the refractive index (n=3) of microemulsions was analyzed at 25 °C with the Abbe Refractometer model B&C 32400 previously calibrated with distilled water.

Viscosity

Viscosity (n=3) was determined at 25 °C with a Brookfield brand Helipath-coupled viscometer model DV-II, with 96 spindles at 60 rpm.

Electrical conductivity

MEs 2A, 2E, 10B, 10C, 16B, 16C and 22B were selected because of their smaller diameter and higher

concentration of S+ Co-S. Conductivity (n=3) was measured at 22 °C using an HI-9835 conductivity meter (Hanna Instruments, USA).

Physical stability test carried out by centrifugation

ME droplet aggregation may result in phase separation that causes irreversible damage. Kinetic instability such as creaming, settling, or any other form of phase separation has been observed by centrifugation (Singh *et al.*, 2017). MEs 2A, 2E, 10B, 10C, 16B, 16C and 22B (n=3) were centrifuged at 3,000 rpm for 30 minutes and at 10,000 rpm for 30 minutes with an NT810 centrifuge (Novatécnica, Brasil). The absence of any phase separation of the ME determined by visual observation was used as a physical stability parameter.

Preparation and Characterization of ME containing PpIX

The preparation of ME containing PpIX was carried out as described above; however PpIX was added to the oily phase to reach a final PpIX concentration of 60 µg/ml after water addition to form 5 g of the ME.

Due to their smaller diameter, MEs O/A (2A), BC (10B), and A/O (16B) were chosen for PpIX incorporation and characterization as follows:

Determination of PpIX content in Me (%)

After 1:200 dilution in DMSO, MEs (n=3) were centrifuged at 3,000 rpm for 10 minutes in an NT810 centrifuge (Novatécnica, Brazil). The supernatant was then collected and PpIX was quantified with an FP 6300 Spectrofluorimeter (JASCO) under the conditions described above in the *Spectrofluorimetric assay* section.

Other analyses such as pH, size/PDI, and ZP (as described for blank MEs) were carried out in ME- PpIX samples previously diluted 1:500 in distilled water.

In vitro release studies

The selected MEs 2A, 10B, and 16B were submitted to the *in vitro* release evaluation in modified Franz cells

(n=6; area= 1.77 cm²) using a hydrophobic Fluoropore membrane (Polytetrafluoroethylene, 0.5 µm pores 47 mm in diameter, Millipore®). Each Franz cell consisted of a 100 mL glass beaker to which 50 mL of the acceptor solution (AS) were added for the solubilization of PpIX for the maintenance of the sink condition according to a previously employed methodology (Rossetti *et al.*, 2010; Da Silva *et al.*, 2013).

The solubility of PpIX in AS was previously found to be 69.14 ± 0.65 µg.mL⁻¹. Two-hundred µL aliquots of each ME, as well as the control (PpIX at 60 µg/mL in the AS) were applied to the membranes and the system was kept at 37 °C under constant stirring at 300 rpm for 24 hours. Aliquots (2 mL) were collected from the AS at 1, 2, 4, 6, 8, and 24 h, with the same volume of new AS being replaced at each time and analyzed for PpIX content released from ME or control solution in the spectrofluorimetric assay. The *in vitro* drug release profile was determined by correlating the drug released (%) for each group *versus* time (h).

In vitro permeability studies

ME 2A (O/W) 10B (BC) and 16B (W/O), were submitted to *in vitro* skin retention and permeation tests in modified Franz cells (n=6 for each group) using porcine ear skins as a membrane. Fifty mL of AS were added to each Franz cell and the skins were attached to the support with the epidermis facing upwards. Two-hundred µL aliquots of the ME and the control (PpIX at 60 µg/mL in PEG 300) were applied to the epidermis of the skin fragments. The system was kept at 37 °C in a temperature-controlled bath under shaking at 300 rpm for 4 h. After this period, a 2 mL aliquot of AS was collected to quantify the PpIX permeated through the skin.

PpIX retention in the SC

After 4 h of *in vitro* permeation, samples of porcine ear skin (n=6 for each group) were taken from Franz cells, washed with distilled water to remove excess formulation and attached to a support with the aid of pins with the epidermis facing upwards. The “tape stripping” technique was then carried out (Da Silva

et al., 2013; Rossetti, Depieri, Bentley, 2013) using 15 adhesive tapes (Scotch Book Tape[®], 3M, St. Paul, MN) pressed onto the epidermis for SC removal and subsequent PpIX quantification.

The strips were placed in a Falcon tube containing 4 mL of DMSO and vortexed for 1 minute. The tube was placed in an ultrasound bath at 40 KHz, continuous mode (Q-335D; Quimis, Diadema, SP, Brazil) for 30 min; the solvent was collected into another tube and filtered through 0.2 µm membranes (Millipore[®]). One µl aliquots of filtrate (DMSO medium) containing PpIX were quantified by spectrofluorimetry and the results are reported as the amount of PpIX retained in the SC/area of exposure (µg. cm⁻²).

PpIX retention in the Epidermis + Dermis ([Ep + D]):

For the *in vitro* determination of PpIX retention in the ([Ep + D]), the skin fragments (n=6 for each group) were cut into small sizes and added to a Falcon tube containing 5 mL of DMSO. The mixture was triturated in an Ultra-Turrax homogenizer (T25 digital; IKA[®], Yamato Koriyama Shi, Nara, Japan) at 4000 rpm for 1 min and placed in an ultrasound bath (Q-335D; Quimis, Diadema, SP, Brazil) for 30 min to break the cells. The solution obtained was filtered and 1 mL aliquots in DMSO medium were quantified by spectrofluorimetry. The results are reported as the amount of PpIX retained in the [EP + D] per area of exposure (PpIX µg. cm⁻²).

Evaluation of PpIX Skin Penetration by Confocal Laser Scanning Microscopy (CLSM)

ME 10B was selected for CLSM evaluation based on the results of the *in vitro* retention studies. First, samples (n=3 for each group) of ME 10B, control (PpIX in PEG 300), and blank (untreated skin) were submitted to the *in vitro* skin permeability procedure using porcine ear skin in modified Franz cells. The experimental conditions were those described above for the *in vitro* permeation studies. After 4 h, the skins were removed from the Franz cells and

washed with distilled water to remove excess formulation. Small rectangles were cut from the center of each skin fragment and placed in small aluminum holders filled with Tissue-Tek[®] O.C.T. Compound (Sakura[®] Finetek).

The samples were frozen with a Leica CM3000 cryostat and cut into 10 µm-thick sections at -20 °C. Glass slides coated with poly-L-lysine (Sigma Aldrich[®] (St. Louis, MO) were prepared for further analysis under a Confocal Microscope. The laser used PpIX excitation at λ of 405 nm and red fluorescence emission at λ 590 to 690 nm. All images were acquired with a resolution of 512 x 512 pixels, 75% laser transmittance, optical cuts of 0.7 depth, and 1 min of scanning time at the same detector gain value, according to the methodology described by de Oliveira Miguel *et al.* 2020.

STATISTICAL ANALYSIS

Results are reported as means ± SD. Data were analyzed statistically by the parametric unpaired two-tailed Student t-test for comparison of two experimental groups. One-way ANOVA (Tukey's multiple comparison test) was used to compare three or more groups, with the level of significance set at P < 0.05.

RESULTS AND DISCUSSION

Preparation of blank MEs

Pseudo Ternary Phase Diagrams (PPD)

The percentage of the components and phases formed under various experimental conditions were determined graphically by PPD, elaborated from the combination of three components, i.e., S+Co-S mixture, oil phase and, aqueous phase (Apolinário *et al.*, 2020).

Figure 1 shows the PPD of the regions of microemulsion formation observed with 10-20% of the aqueous phase, 10-50% of the oily phase, and 40%-80% of the S+ CoS mixture. The points correspond to ME1, ME2, ME 9, ME 16, ME 22, and ME27.

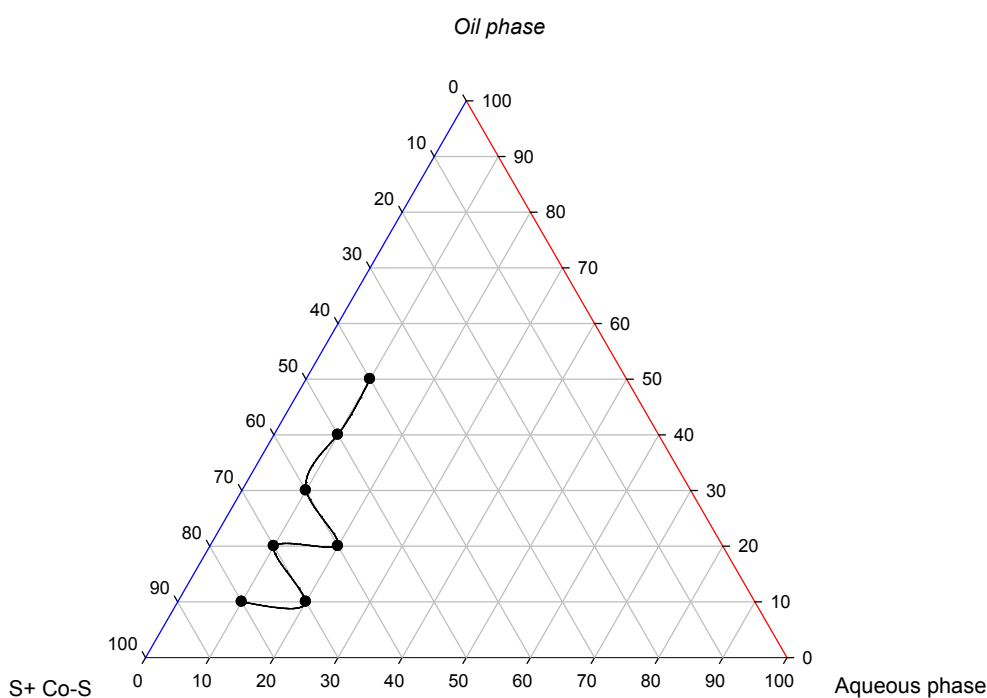


FIGURE 1 - Pseudo-ternary phase diagrams obtained with the formed microemulsions ME 1, ME 2, ME 9, ME 10, ME 16, ME 22 and ME 27. The X (black line), Y (red line) and Z (blue line) axes represent the aqueous phase, oil phase and S+Co-S mixture, respectively.

Blank ME characterization

(PZ), Refractive Index (RI), and Viscosity (cp) and the results are shown in Table III.

Blank ME were selected (Table II) for characterization regarding size/PDI, pH, Zeta Potential

TABLE III - Mean values of pH, Refractive Index (RI), Viscosity (cp), Diameter (nm), Zeta Potential (PZ) and Polydispersion Index (PDI) (n = 3 for each group) from blank ME 2, ME 10, ME 16 and ME 22 (without PpIX)

ME	Name	pH± S.D	R.I	Viscosity (cp)	Size (nm±S.D)	PDI± S.D	ZP (mV) ± S.D
	2A	5.53 ± 0.374	1.45	469 ± 2.455	162.8 ± 0.866	0.5 ± 0.007	-32 ± 1.210
	2B	5.62 ± 0.438	1.43	329 ± 1.345**	178.3 ± 2.159	0.4 ± 0.006	-37 ± 9.151
O/A	2C	5.37 ± 0.261	1.42	282 ± 0.98**	248.7 ± 4.813	0.5 ± 0.035	-28 ± 1.844
	2D	5.45 ± 0.318	1.42	329 ± 3.540**	565.9 ± 14.868**	0.5 ± 0.071	-36 ± 1.504
	2E	4.78±0.156**	1.41**	361 ± 2.430**	535.9 ± 23.674**	0.5 ± 0.047	-46 ± 1.106*
	10A	5.04 ± 0.028	1.44	1700 ±10.250	319.3 ± 13.151	0.5 ± 0.048	-47 ± 2.000
	10B	5.01 ± 0.007	1.44	1850 ±11.750**	301.4 ± 16.643	0.6 ± 0.051	-29 ± 0.550**
BC	10C	4.93 ±0.049	1.43	344 ± 0.890**	367.0 ± 19.410	0.6 ± 0.091	-35 ± 4.44*
	10D	4.76 ± 0.169	1.35	329 ± 1.345**	435.1 ± 40.711	0.9 ± 0.210*	-40 ± 2.193

TABLE III - Mean values of pH, Refractive Index (RI), Viscosity (cp), Diameter (nm), Zeta Potential (PZ) and Polydispersion Index (PDI) (n = 3 for each group) from blank ME 2, ME 10, ME 16 and ME 22 (without PpIX)

ME	Name	pH± S.D	R.I	Viscosity (cp)	Size (nm±S.D)	PDI± S.D	ZP (mV) ± S.D
	10E	4.47 ±0.021	1.77**	312 ± 3.450**	435.8 ± 6.718	0.6 ± 0.031	-41 ± 1.473
	16A	5.00 ± 0.000	1.46	422 ±1.560	288.4 ± 2.739	0.5 ± 0.039	-43 ± 3.066
	16B	4.97 ± 0.021	1.41	548 ± 3.650**	383.6 ± 6.819	0.6 ± 0.029	-48 ± 3.516
A/O	16C	4.89 ± 0.077	1.43	501 ± 0.560**	385.8 ± 42.552	0.9 ± 0.097*	-43 ± 1.137
	16D	4.83 ± 0.120	1.43	391 ±0.446**	834.2 ± 132.646**	0.8 ± 0.191	-47 ± 8.386
	16E	4.76±0.169	1.42	344 ± 0.848**	517.5 ± 100.524**	0.8 ± 0.239	-62 ± 0.200**
	22A	4.52±0.014	1.43	361 ±0.890	635.1 ± 41.454	1.0 ± 0.000	-59 ± 0.871
	22B	4.36±0.099	1.42	329 ± 0.786**	730.8 ± 42.733	1.0±0.000	-50 ± 5.565

Statistical analysis was performed using ANOVA followed by the Tukey's multiple comparison test. Asterisks indicate a significant difference inside a group (O/A, BC or A/O). Differences were considered significant for: **pH**: 2A vs 2E (p < 0.01**); **I.R.**: 10A vs 10E (p < 0.001 **); **viscosity**: 2A vs 2B, 2C, 2D, 2E (p < 0.001**); 10A vs 10B, 10C, 10D and 10E (p < 0.001**); 16A vs 16B, 16C, 16D, 16E (p < 0.001**); 22A vs 22B (p < 0.001**); **size**: 2A vs 2D and 2A vs 2E (p < 0.001**); 16A vs 16D, 16E (p < 0.001**); **P.D.I.**: 10A vs 10D and 16A vs 16C (p < 0.01*); **Z.P.**: 2A vs 2E (p < 0.01*), 10A vs 10B (p < 0.001**), 10A vs 10C (p < 0.05*), 16A vs 16E (p < 0.001**).

pH Measurements

For all blank MEs the pH values were close to the skin pH (~4.5-6.5) (Ali, Yosipovitch, 2013), indicating that MEs are suitable for topical application.

Refractive index (RI)

The refractive index (RI) is a characteristic optical variable that controls light propagation in the medium. Microemulsions are transparent or translucent since their droplet diameter is less than ¼ of the wavelength of light, so that they scatter little light. (Agrawal, Agrawal, 2012). The RI values were used for size measurements and ranged from 1.35 to 1.77, in agreement with the literature (de Campos Araújo, Thomazine, Lopez, 2010; Chauhan, Muzaffar, Lohia, 2013).

Viscosity determinations

Viscosity influences the stability, application/maintenance on the skin during use, and drug release of ME (Nastiti *et al.*, 2017). In general, viscosity (Table III) varied according to the type of ME formed, in the range of 282 to 1850 cp, ranging from 282 to 469 cp for ME 2

(O/A), from 329 to 548 cp for ME 16 and 22 (A/O), and from 312 to 1850 cp for ME 10 (BC).

The viscosity of MEs is a function of the components and concentrations of surfactants, water, and oil in the formulation. When the percentage of the oil phase (10%, 20%, 30%, and 40%) was increased there was no proportional increase in viscosity. Likewise, decreasing the percentage of the aqueous phase from 20% to 10% and increasing the percentage of S+Co-S from 50% to 70% did not cause a significant increase in viscosity. In general, the least viscous ME was ME 2C (O/W; 282 cp) and the most viscous one was 10 B (BC; 1850 cp), respectively 10% and 20% of the oil phase. This indicates that the proportion of components should influence the final viscosity. The importance of viscosity for MEs resides in skin application without running, stability, and drug release (Nastiti *et al.*, 2017).

Size and PDI

MEs showed sizes in the nanometric range (162.8 to 834.2 nm) (Table III). The smallest size was found for O/A ME 2A (162.8 nm) at 70% of S+ Co-S (3:1), that is, S in greater quantity compared to Co-S.

It is known that droplet size tends to decrease with increasing S concentration and with the addition of a Co-S to the system. Overall, the ME size results agree with this assumption, since higher percentages of surfactant (75%) produced smaller MEs. This size tends to increase up to 25% as the percentage of surfactant decreases (Formariz *et al.*, 2005). Table III shows that size increased when the percentage of the S+ Co-S mixture decreased to 60% (MEs 10 and 16) and when the proportion of S was smaller than that of Co-S. Thus, the size of ME O/A 16D (834.2 nm) was largest at 60% S+ Co-S (1:2 or 33.33%:66.66%).

The polydispersity index (PDI) measures the uniformity of particle size distribution, so that values smaller than 0.05 are considered highly monodisperse. PDI values may vary from 0.01 (monodispersed particles) to 0.5-0.7, whereas a PDI value > 0.7 indicated broad particle size distribution of the formulation (Danaei *et al.*, 2018). Table III shows PDI 0.5- 0.6 for most of the MEs evaluated. Since MEs 22A and 22B showed a PDI=1.0 they were not included in the *in vitro* assays.

Superficial charge or Zeta potential (ZP)

This parameter indicates physical stability, and a ZP greater than ± 30 mV is necessary for excellent electrostatic stabilization (Bedin, 2011). Among the ME, ZP ranged from -28 mV to -62 mV (Table III), indicating colloidal stability due to the high energy barrier between particles (Bhattacharjee, 2016).

Electrical conductivity

Selected MEs such as 2 (A and E), 10 (B and C), 16 (B, C), and 22B were used to evaluate this parameter to determine aqueous or oily continuous domains in a micro emulsified system (Rossi *et al.*, 2007). The increase in the electrical conductivity of MEs characterizes their internal structure (Lopes, 2014); thus, as water content increases, the electrical conductivity of the system also increases. MEs with higher water concentration (20% in ME 2 and ME 10) had higher conductivity values (8.24 to 9.74 $\mu\text{S}/\text{cm}$) compared to samples with lower water concentration (10% in ME 16 and ME 22) ranging from 2.30 to 3.63 $\mu\text{S}/\text{cm}$ (Table IV).

Physical stability by centrifugation

Under the conditions analyzed, no ME showed visual phase separation after centrifugation, demonstrating good physical stability (Singh *et al.*, 2017).

TABLE IV - Electrical conductivity of selected formulations (without PpIX)

Formulations	Electrical conductivity ($\mu\text{S}/\text{cm}$)
2A (O/A)	9.56
2E (O/A)	9.74
10B (BC)	8.24
10C (BC)	8.92
16B (A/O)	3.63 *
16C (A/O)	3.63 *
22B (A/O)	2.30 *

Statistical analysis was performed using ANOVA followed by the Tukey's multiple comparison test. Differences were considered significant to $p < 0.01$ *. Asterisks indicate a significant difference compared to ME 2A.

ME Characterization After PpIX incorporation

After PpIX incorporation, MEs 2A, 10B, and 16B were assayed for drug content (%), pH, size, PDI, PZ, *in vitro* release studies, *in vitro* permeation studies and Confocal Microscopy.

Percentage of PpIX in the ME

Approximately 80% of PpIX was encapsulated from MEs (n=3 for each group), with similar values (no significant difference) among MEs 2A, ME 10B and ME16B (80.6%, 79.6% and 84.6% respectively). These values are considered suitable for micro/nanostructured systems.

pH

The pH of a topical formulation should be close to the skin's pH (4.56.5) to avoid local irritation (Ali, Yosipovitch, 2013). The pH values of the MEs selected

in the absence and presence of PpIX (Table V) were not significantly changed, remaining in the skin pH

range, which indicates that MEs are suitable for topical application.

TABLE V - Mean values of pH, diameter (nm), Polydispersity Index (PDI) and Zeta Potential (PZ) (n = 3 for each group) before (MEs- blank) and after PpIX incorporation (MEs- PpIX)

Formulations	pH (blank/ME-PpIX)	Size (nm) (blank± S.D /ME-PpIX± S.D)	PDI (blank± S.D /ME-PpIX± S.D)	ZP (mV) (blank/ME-PpIX)
ME 2A	5.53 ± 0.374	162.8 ± 0.866	0.5 ± 0.057	-32 ± 1.210
	5.83 ± 0.200	162.1 ± 0.808	0.5 ± 0.006	-33 ± 1.000
ME 10B	5.01 ± 0.007	301.4 ± 16.643	0.6 ± 0.010	-29 ± 0.550
	5.33 ± 0.350	359.9 ± 3.330	0.7 ± 0.062	-30 ± 0.450
ME 16B	4.97 ± 0.021	383.6 ± 6.819	0.6 ± 0.057	-48 ± 3.516
	4.91 ± 0.030	605.0 ± 68.703**	0.7 ± 0.103	-40 ± 2.890

Statistical analysis was performed using ANOVA followed by the Tukey's multiple comparison test. Asterisks indicate a significant difference inside a group (ME 16B). Differences were considered significant for size to ME 16B blank vs ME 16B after PpIX incorporation ($p < 0.001^{**}$).

Size, PDI, and PZ

There was no significant change in the diameter of ME 2A or ME 10B after PpIX addition (~162nm and 360 nm respectively), while size increased significantly in ME 16B (383 nm to 605 nm; $** p < 0.001$).

A significant increase in the size of nanostructured systems after drug incorporation can be disadvantageous. However, using the topical route can improve the local effect of drugs and minimize systemic absorption. Indeed, the objective is that MEs should facilitate the transport of active agents through skin structures by interacting with skin lipids and allowing drug deposits in the skin for sustained release (Hathout *et al.*, 2010). For example, several studies have shown that MEs enhance the topical delivery of drugs such as ketoconazole (Patel *et al.*, 2011) dithranol (Raza *et al.*, 2011) terbinafine hydrochloride (Dabhi *et al.*, 2011), tretinoin (Khanna, Katare, Drabu, 2010), and 5-ALA for PDT (De Campos Araújo, Thomazine, Lopez, 2010).

PDI values ranged from 0.5-0.7 for MEs containing PpIX such as ME 2A, 10B, and 16B (Table V) and are

acceptable values indicating monodisperse samples, as mentioned before.

The zeta potential (ZP) ranged from -30 to -40 mV for ME 2A, 10B, and 16B, with little change compared to blank ME (Table V), showing that PpIX incorporation does not change the initial electrostatic stability.

In vitro PpIX release

In vitro release studies were carried out to assess PS release from MEs and its reproducibility from batch to batch. Among several factors (solubility, percent drug content, etc.), the rate of drug release in a delivery system depends upon its size, so that decreased particle sizes often result in higher release of hydrophobic drugs (Kogan, Garti, 2006; Fanun, 2012).

The results of the *in vitro* release evaluations (Figure 2) showed that the control solution (60 µg/ml in PpIX in PEG 300) achieved a PpIX release rate of ~90% in 24 h, while MEs 2A, 10B, and 16B showed a release of ~70%, 30%, and 10%, respectively, characterizing appropriate drug delivery systems.

After 4 h, lower rates of PpIX release were observed for control ~ 60% PpIX as compared to rates of ~25%, 3.8% and 1.5% for MEs 2A, 10B, and 16B, respectively.

Literature data show that the *in vitro* drug release rate from a delivery system is inversely proportional to both viscosity and droplet size, so that percent drug release can increase in the presence of small particle size

and low viscosity (Formariz *et al.*, 2005). Similarly, ME 2A had the smallest diameter (162.1 nm) among the three formulations (359.9 and 605 nm, respectively, for ME 10B and 16B). In this case, small size could contribute to the higher percent release of PpIX. However, no significant difference in percent PpIX release was observed between 10B and 16B despite differences in size.

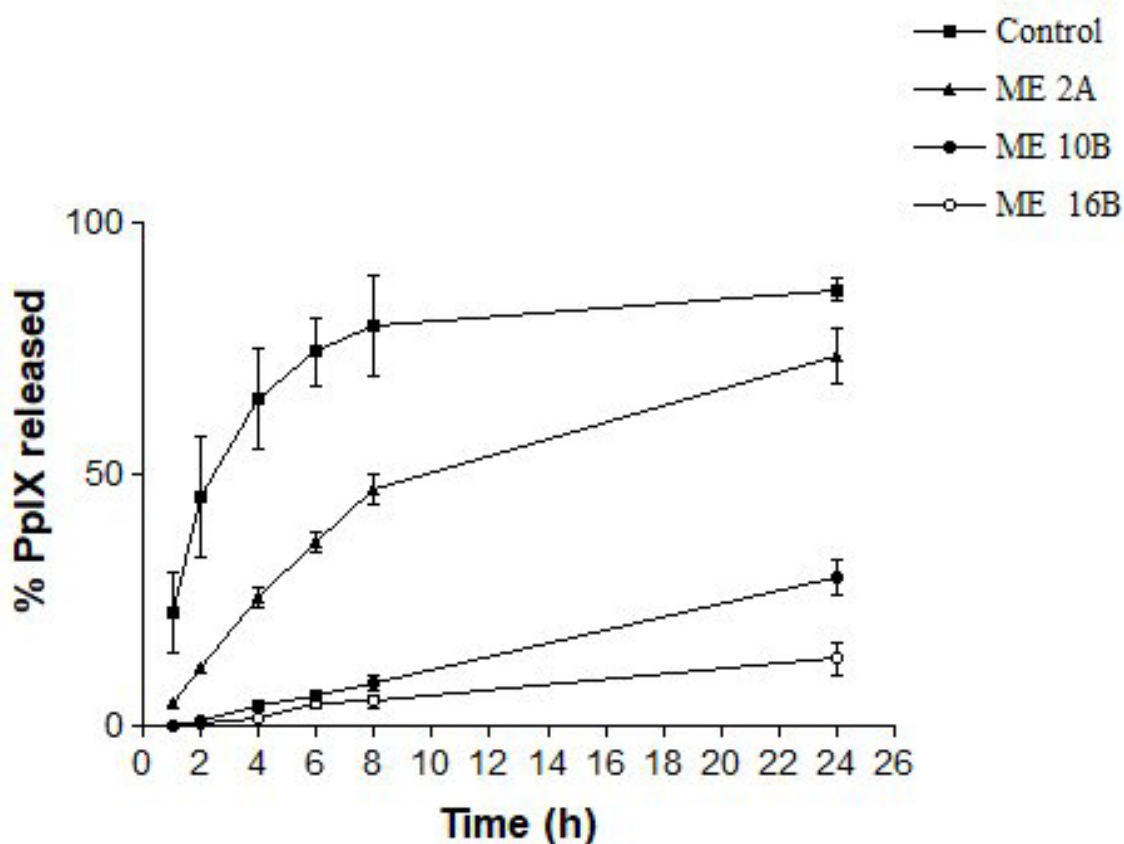


FIGURE 2 - *In vitro* release profile of PpIX (60 µg/mL) – Control; ME 2A; ME 10B and ME 16B (n=6 for each group) Statistical analysis: One-way ANOVA. P value < 0.0001. **4 h**: Difference considered significant (**p<0.001) for control *versus* ME 2A, 10B and ME 16B. Nonsignificant (p> 0.05) for ME 10B *versus* ME 16B. **24h**: Difference considered nonsignificant (p> 0.05 in 24 h) between control and ME 2A. Difference considered significant (**p<0.01) within 24 h for control *versus* ME 10B and ME 16B and *p<0.05 for ME 10B *versus* ME 16B.

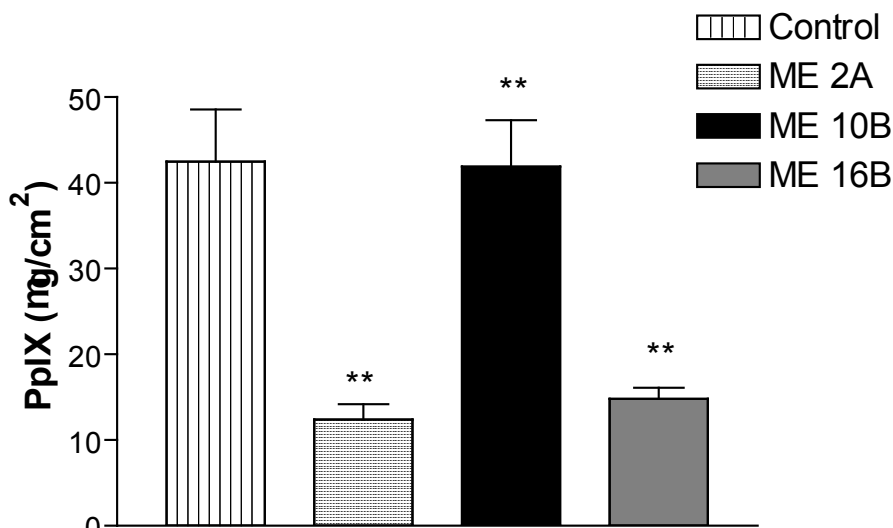
In vitro permeability studies:

None of the MEs (2A, 10B, or 16B) promoted PpIX permeation through the skin, with no measurable amounts observed in the acceptor solution. Skin retention studies

(SC and EP+D) of PpIX (Figure 3) were performed to assess whether MEs are suitable for topical application.

In the SC (Figure 3A), PpIX retention of control solution or ME 10B was similar and ~4-fold higher compared to MEs 2A and 16B.

(A)



(B)

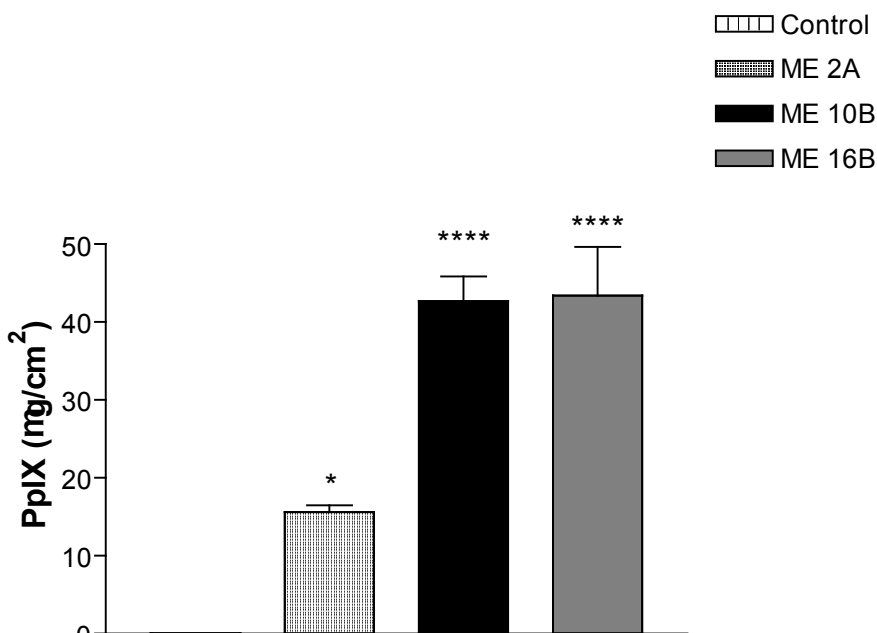


FIGURE 3 - *In vitro* PpIX retention in the SC (n= 6 for each group) (A) after 4 h of the *in vitro* permeability study. Statistical analysis: One-way ANOVA. Difference considered significant (**p < 0.01) between Control and ME 2A and ME 16B. Difference considered nonsignificant (p > 0.05) between Control and ME 10B (B) Epidermis + Dermis ([Ep+D]) from ME (n= 6 for each group). Statistical analysis: One-way ANOVA. The control bar is absent in the graph because PpIX was below the detection limit. Difference considered significant (*p < 0.05) between control and ME 2A. Difference considered significant (****p < 0.001) between Control and ME 10B and ME 16B.

In the [Ep+D] (Figure 3B), ME 10B and 16B achieved the highest PpIX retention (~3 and ~40 fold higher than ME 2A and the control solution, respectively).

The control solution did not retain measurable amounts of PpIX (without bar). It is worth emphasizing that both ME 10B and 16B have high percentages of surfactants

in their compositions (60% of the total S+CoS mixture at a proportion of 2:1, or 66.6% and 33.3%).

The main advantage of MEs for topical application is the increased penetration of drugs into the skin, for which several mechanisms have been proposed. The literature reports several combined mechanisms rather than one to clarify such an effect; for instance, the high proportion of *surfactants and oil phase* components of the system, and the presence of *penetration enhancers* (Baroli *et al.*, 2000).

Such factors can disturb the organized lipid structure of the SC, breaking the skin barrier or increasing the solubility of the active agent in the skin (increased skin/vehicle partition coefficient) (El Maghraby, 2008). As shown in Figure 3B, a significant increase in the skin PpIX retention for both ME 10B and ME 16B can be related to the enhancer effect of the micro emulsified system which could be due to the high percentage of S+Co-S (60%) and oleic acid (20% and 30%, respectively).

As previously mentioned, ME 16B encapsulated PpIX had a diameter \sim 2 times larger than ME10B. However, the retained amounts of PpIX were similar in [Ep+D] (Figure 3B), possibly indicating that size had little influence on retention in Ep+D and demonstrating the penetration enhancer effect of oleic acid (20-30%) along with the high percentage of the S: Co-S mixture (60%) in both formulations. This means that the “mixing” of ME components can increase the penetration of PpIX into the skin compared to individual ones, promoting greater efficiency.

ME 10B and 16B released less PpIX than ME 2A and control (Figure 2) at 4 h (time of skin retention assays) but showed the highest retention in [Ep+D]. (Figure 3B). Again, increased PpIX retention in the [Ep+D] appears to be more related to the composition of the ME than to the release rate or droplet size of the MEs.

The oil phase components, like fatty acids, can contribute to increased drug retention in the skin due to a penetration enhancer effect (Kogan, Garti, 2006). In the current work, oleic acid was the oil phase for MEs. It is a cis-unsaturated free fatty acid abundantly found in nature, including human skin, and recognized by several *in vitro* studies as an efficient skin penetration enhancer (Pierre *et al.*, 2006). This substance causes changes in

SC lipid packaging, inducing phase separation (Hathout *et al.*, 2010).

Other studies have shown oleic acid as a penetration enhancer for cutaneous delivery of drugs for PDT of skin tumors such as 5-ALA (Pierre *et al.*, 2006; Carollo., 2007) and chloroaluminum phthalocyanine (Almeida *et al.*, 2018). Other drugs such as celecoxib (Quiñones *et al.*, 2014) also showed increased *in vitro* and *in vivo* skin penetration and/or permeation in the presence of oleic acid.

Still, ME can increase skin hydration and consequently increase penetration/retention of active agents (Williams, Barry; 2012). Oil phase compounds can have occlusive properties on the skin since they prevent water evaporation from the skin surface, increasing the water content of the skin (Patzelt *et al.*, 2012) and consequently drug penetration. Again, OA, a fatty acid present in high percentage in MEs, may favor the occlusive property. Another factor is the high capacity of MEs to carry drugs compared to unstructured vehicles (Kreilgaard, 2002).

In this sense, MEs can be an alternative for carrying PpIX in the skin to increase (i) aqueous solubility and consequently decrease water aggregation without losing the photodynamic effect and (ii) PS skin retention (De Campos Araújo, 2010), mainly for nodular tumors containing a thick layer of SC that hinders PS absorption into the skin.

Another aspect of the development of MEs is the selection of a surfactant (S) and co-surfactant (Co-S). Combinations that effectively reduce interfacial tension produce stable MEs with appropriate particle sizes. Furthermore, the components must ensure minimal skin irritation. In the current study, we used Tween 80[®], a non-ionic surfactant widely employed in many pharmaceutical formulations as a non-toxic and non-irritating substance (Kaur, Mehta, 2017).

Confocal Laser Scanning Microscopy (CLSM)

CLSM is an imaging tool for the study of the location of PS applied to the skin. Using fluorescence probes, it is possible to assess PS interaction with the biological system, depth, and penetration pathways in the

skin (Rossetti, Depieri, Bentley, 2013). For the present study, ME 10B (n=3) was selected because of its excellent characteristics of pH, size, ZP, slow-release profile (30% at 24h), and significantly increased cutaneous retention in EP+D.

PpIX penetration depth was determined by CLSM after 4 h of *in vitro* skin permeation. Greater fluorescence intensity in deeper layers of the skin (dermis) means an advance for PDT of skin tumors since the effectiveness

of this therapy depends on the concentration of PS in the target tissue. Photomicrographs (Figure 4) show that the fluorescence uptake of PpIX in the epidermis (including SC) was higher than in the dermis for all groups. However, control samples (Figure 4A) showed higher fluorescence in the epidermis compared to ME 10B (Figure 4B) and blank (Figure 4C). In the Dermis, ME 10B had some PpIX fluorescence points (Figure 4B), indicating PS penetration into this deeper layer.

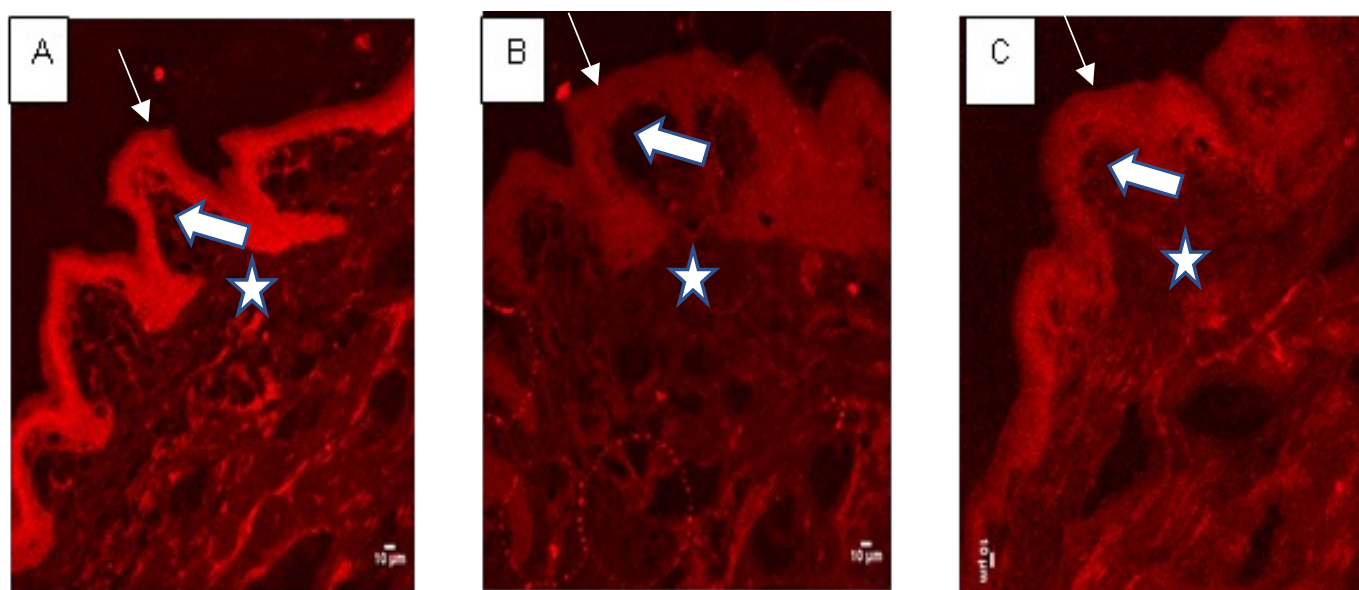


FIGURE 4 - Photomicrograph of skin samples representing the fluorescence intensity captured by confocal microscopy after 4 h of the *in vitro* permeation experiments with: (A) positive control, (B) ME10B and (C) negative control (blank), n=3 for each sample. Thin arrow: stratum corneum; thick arrow: epidermis; star: dermis.

Despite the low fluorescence intensity, this result agrees with the *in vitro* retention results (Figure 3B), i.e., higher PpIX retention in the dermis than in control solution. It is most probable that ME 10B permitted higher skin penetration because PpIX remained on the SC surface (Figure 3A) of furrows or hair follicles from where PpIX skin partition to deeper skin layers was favorable, as shown in Figure 3B. Thus, PpIX was preferentially retained in SC, which acted as a PpIX deposit for subsequent penetration into the underlying layers (dermis), as seen in Figures 3B and 4B.

After 4 h of the *in vitro* skin retention and CLSM experiments, the release of PpIX (Figure 2) was about 60% for the control and less than 4% for ME 10B.

Even so, higher PpIX retention in the dermis was observed (Figures 3B and 4B) from ME 10B, demonstrating the “enhancer” effect of the ME compared to control. The small mean diameter of ME 10B (~360 nm) associated with the presence of OA may have contributed to the higher retention of PpIX in the dermis compared to control, as discussed above. This would result in greater efficacy for the topical application of ME 10B associated with PDT of skin tumors. In addition, it would represent a great advantage since highly lipophilic PpIX would not

be efficiently retained in the dermis (action site for PDT) in skin tumors without the proposed ME.

CONCLUSION

According to the methodologies used and the results obtained, ME 10B (BC) has the potential for topical application in the PDT of skin tumors since it showed (i) high *in vitro* PpIX retention both in the SC and in the [Ep + D] (ii) size on a nanometric scale with the addition of PpIX (~360 nm), and (iii) high PZ (-29.0) and good stability by decreasing the aggregation tendency of ME droplets (iv), pH 5.3, being compatible with human skin, (v) having high viscosity (1850 cp) that prevents draining during application and (vi) PpIX release ~ 30% within 24 h, and thus showing a slower release profile. Furthermore, microemulsions can reduce PpIX aggregation in aqueous media and consequently inhibit the generation of dimers (harmful to singlet oxygen generation) and then contribute to the photodynamic effect of PpIX.

FUTURE PERSPECTIVES

The next step will be to carry out ME 10B assays in cultured non-melanoma skin cancer cells (squamous cell carcinoma) to determine whether ME interferes with the photodynamic efficiency of PpIX after light incidence (PDT).

ACKNOWLEDGMENTS

Thanks are due to Programa Institucional de Bolsas de Iniciação Científica (PIBIC) for granting a Scientific Initiation Scholarship to Paula Ângela de Souza Marinho Leite.

REFERENCES

- Agrawal OP, Agrawal S. An overview of new drug delivery system: microemulsion. *Asian J Pharm Sci Tech*. 2012;2(1):5-12.
- Ali SM, Yosipovitch G. Skin pH: from basic science to basic skin care. *Acta Derm Vener*. 2013;93(3):261-269.
- Almeida EDP, Dipieri LV, Rossetti FC, Marchetti JM, Bentley MVL, Nunes RDS, et al. Skin permeation, biocompatibility, and antitumor effect of chloroaluminum phthalocyanine associated to oleic acid in lipid nanoparticles. *Photodiagn Photodyn Ther*. 2018;2:262-273.
- Apolinário AC, Salata GC, Bianco AF, Fukumori C, Lopes LB. Abrindo a caixa de pandora dos nanomedicamentos: há realmente muito mais espaço lá embaixo. *Quim Nova*. 2020;(43):212-225.
- Baroli B, López-Quintela MA, Delgado-Charro MB, Fadda AM, Blanco-Méndez J. Microemulsions for topical delivery of 8-methoxsalen. *J Controlled Release*. 2000;69(1):209-218.
- Basoglu H, Bilgin MD, Demir, MM. Protoporphyrin IX-loaded magnetoliposomes as a potential drug delivery system for photodynamic therapy: fabrication, characterization, and *in vitro* study. *Photodiagn Photodyn Ther*. 2016;13:81-90.
- Bhattacharjee S. DLS and zeta potential—what they are and what they are not? *J Controlled Release*. 2016;235:337-351.
- Bedin AC. Nanoemulsões contendo benzoilmetronidazol: desenvolvimento, caracterização e estudo de liberação *in vitro*. [dissertação]. Santa Catarina: Universidade Federal de Santa Catarina, 2011.
- Bonnet, R. Photosensitizers of porphyrins and phthalocyanine series for photodynamic therapy. *Chem Soc Rev*. 1995;24:19-33.
- Calixto GMF, Bernegossi J, De Freitas LM, Fontana CR, Chorilli M. Nanotechnology-Based drug delivery systems for photodynamic Therapy of Cancer: A review. *Molecules*. 2016;(21):342.
- Carollo ARH. Influência do ácido oléico como promotor de absorção cutânea para o ácido 5- aminolevulínico na terapia fotodinâmica do câncer de pele: estudos *in vitro* e *in vivo* em modelo animal. [dissertação]. São Paulo: Universidade de São Paulo, Faculdade de Ciências Farmacêuticas de Ribeirão Preto; 2007.
- Chauhan LALIT, Muzaffar FAIZI, Lohia SARITA. Design, development and evaluation of topical microemulsion. *Int J Pharm Pharm Sci*. 2013;5(2):604-610.
- Dabhi MR, Nagori SA, Sheth NR, Patel NK, Dudhrejiya AV. Formulation optimization of topical gel formulation containing micro-emulsion of terbinafine hydrochloride with simplex lattice design. *Micro Nanosyst*. 2011;3(1):1-7.
- Damasceno BPGL, Silva JA, Oliveira EE, Silveira W, Araújo IB, Oliveira AGD. Microemulsão: um promissor carreador para moléculas insolúveis. *Rev Cienc Farm Basica Apl*. 2011;32(1):9-18.
- Danaei M, Dehghankhold M, Ataei S, Hasanzadeh Davarani F, Javanmard R, Dokhani A, et al. Impact of particle size and

- polydispersity index on the clinical applications of lipidic nanocarrier systems. *Pharmaceutics*. 2018;10(2),57.
- Da Silva CL, Del Ciampo JO, Rossetti FC, Bentley MVL, Pierre MBR. Improved *in vitro* and *in vivo* cutaneous delivery of protoporphyrin IX from PLGA-based nanoparticles. *Photochem Photobiol*. 2013;89(5):1176-1184.
- De Campos Araújo, LMP. Dendrímeros como carreadores da protoporfirina IX para a terapia fotodinâmica tópica do câncer de pele. (Tese de doutorado) Universidade de São Paulo (USP). Faculdade de Ciências Farmacêuticas de Ribeirão Preto; 2010.
- De Campos Araújo LMP, Thomazine JA, Lopez, RFV. Development of microemulsions to topically deliver 5-aminolevulinic acid in photodynamic therapy. *Eur J Pharm Biopharm*. 2010;75(1):48-55.
- Deda DK, Araki K. Nanotechnology, Light and chemical action: an effective combination to kill cancer cells. *J Braz Chem Soc*. 2015;26(12):2448-2470.
- de Oliveira Miguel J, da Silva DB, da Silva GCC, Corrêa RJ, de Oliveira Miguel NC, Lione VDOF, et al. Polymeric nanoparticles favor the *in vitro* dermal accumulation of Protoporphyrin IX (PpIX) with optimal biocompatibility and cellular recovery in culture of healthy dermal fibroblasts after Photodynamic Therapy. *J Photochem Photobiol A*. 2020;386:112109.
- da Silva DB, da Silva CL, Davanzo NN, da Silva Souza R, Correa RJ, Tedesco AC, et al. Protoporphyrin IX (PpIX) loaded PLGA nanoparticles for topical Photodynamic Therapy of melanoma cells. *Photodiagn Photodyn Ther*. 2021;35:102317.
- Dögnitz, N, Salomon D, Zellweger M, Ballini JP, Gabrecht T, Lange N, et al. Comparison of ALA-and ALA hexyl-ester-induced PpIX depth distribution in human skin carcinoma. *J Photochem Photobiol B: Biol*. 2008;93(3):140-148.
- Donnelly RF, McCarron PA, Woolfson AD. Drug delivery of aminolevulinic acid from topical formulations intended for photodynamic therapy. *Photochem Photobiol*. 2005;81(4):750-767.
- El Maghraby GM. Transdermal delivery of hydrocortisone from eucalyptus oil microemulsion: effects of cosurfactants. *Int J Pharm*. 2008;355(1-2):285-292.
- Fanun M. Microemulsions as delivery systems. *Curr Opin Colloid Interface Sci*. 2012;17(5):306-313.
- Formariz TP, Urban MCC, Silva Júnior AAD, Gremião MPD, Oliveira, AGD. Microemulsões e fases líquidas cristalinas como sistemas de liberação de fármacos. *Rev Bras Cienc Farm*. 2005;41(3):301-313.
- Harrison SM, Barry BW, Dugard PH. Effect of freezing on human skin permeability. *J Pharm Pharmacol*. 1984;(35):261-262.
- Hathout RM, Mansour S, Mortada ND, Geneidi AS, Guy RH. Uptake of microemulsion components into the stratum corneum and their molecular effects on skin barrier function. *Mol Pharm*. 2010;7(4):1266-1273.
- INCA-Instituto Nacional do Câncer –. Câncer de pele não melanoma [citado 2022 Abril 26]. Available from: <https://www.inca.gov.br/tipos-de-cancer/cancer-de-pele-nao-melanoma>.
- Kaur G, Mehta SK. Developments of Polysorbate (Tween) based microemulsions: Preclinical drug delivery, toxicity and antimicrobial application. *Int J Pharm*. 2017;529(1-2):134-160.
- Khanna S, Katare OP, Drabu S. Lecithinised microemulsions for topical delivery of tretinoin. *Int J Drug Dev Res*. 2010;2(4):711-9.
- Kloek J, Akkermans W, Van Henegouwen GMJB. Derivatives of 5-aminolevulinic acid for photodynamic therapy: enzymatic conversion into protoporphyrin. *Photochem Photobiol*. 1998;67(1):150-154.
- Kogan A, Garti N. Microemulsions as transdermal drug delivery vehicles. *Adv Colloid Interface Sci*. 2006;(123):369-385.
- Kreilgaard, M. Influence of microemulsions on cutaneous drug delivery. *Adv Drug Deliv Rev*. 2002;54(Suppl 1):S77-S98.
- Lopes LB. Overcoming the cutaneous barrier with microemulsions. *Pharmaceutics*. 2014;6(1):52-77.
- McLoone N, Donnelly RF, McCarron PA, Walsh M, McKenna K. Aminolevulinic acid penetration into nodular basal cell carcinomas: influence of different concentrations and application times on amounts of ala delivered via a bioadhesive patch. *Clin Photodyn*. 2004;1:5-6.
- Nastiti CM, Ponto T, Abd E, Grice JE, Benson HA, Roberts MS. Topical nano and microemulsions for skin delivery. *Pharmaceutics*. 2017;9(4):37.
- Patel MR, Patel RB, Parikh JR, Solanki AB, Patel BG. Investigating effect of microemulsion components: *in vitro* permeation of ketoconazole. *Pharm Dev Technol*. 2011;16(3):250-8.
- Patzelt A, Lademann J, Richter H, Darvin ME, Schanzer S, Thiede G, et al. *In vivo* investigations on the penetration of various oils and their influence on the skin barrier. *Skin Res Technol*. 2012;18(3):364-369.

Pierre MBR, Ricci E, Tedesco AC, Bentley MVLB. Oleic acid as optimizer of the skin delivery of 5-aminolevulinic acid in photodynamic therapy. *Pharm Res.* 2006;23(2):360-366.

Raza K, Negi P, Takyar S, Shukla A, Amarji B, Katare OP. Novel dithranol phospholipid microemulsion for topical application: development, characterization and percutaneous absorption studies. *J Microencapsul.* 2011;28(3):190-9.

Qidwai A, Nabi B, Kotta S, Narang JK, Baboota S, Ali J. Role of nanocarriers in photodynamic therapy. *Photodiagn Photodyn Ther.* 2020;30:101782.

Quiñones OG, Mata dos Santos HA, Kibwila DM, Leitao A, dos Santos Pyrrho A, Pádula MD, et al. *In vitro* and *in vivo* influence of penetration enhancers in the topical application of celecoxib. *Drug Dev Ind Pharm.* 2014;40(9):1180-1189.

Rossetti FC, Depieri LV, Tedesco AC, Bentley MVLB. Fluorometric quantification of protoporphyrin IX in porcine skin and phosphate buffer samples from *in vitro* penetration/permeation studies. *Braz J Pharm Sci.* 2010;46(4):753-760.

Rossetti FC, Depieri LV, Bentley MVLB. Confocal laser scanning microscopy as a tool for the investigation of skin drug delivery systems and diagnosis of skin disorders. Confocal laser microscopy-principles and applications in medicine, biology, and the food sciences. 2013;99-140.

Rossetti FC, Depieri L, Praça FG, Del Ciampo JO, Fantini MC, Pierre MBR, et al. Optimization of protoporphyrin

IX skin delivery for topical photodynamic therapy: nanodispersions of liquid-crystalline phase as nanocarriers. *Eur J Pharm Sci.* 2016;83:99-108.

Rossi CGFT, Dantas TDC, Neto AAD, Maciel MAM. Microemulsões: uma abordagem básica e perspectivas para aplicabilidade industrial. *Rev Univ Rural Ser Cienc Exatas Terra.* 2007;26(1-2):45-66.

Silva JAD, Apolinário AC, Souza MSR, Damasceno BDL, Medeiros ACD. Administração cutânea de fármacos: desafios e estratégias para o desenvolvimento de formulações transdérmicas. *Rev Cienc Farm Basica Apl.* 2010;31(3):125-131.

Singh Y, Meher JG, Raval K, Khan FA, Chaurasia M, Jain NK, et al. Nanoemulsion: Concepts, development, and applications in drug delivery. *J Control Rel.* 2017;252:28-49.

Wachowska M, Muchowicz A, Firczuk M, Gabrysiak M, Winiarska M, Wańczyk M. Aminolevulinic acid (ALA) as a prodrug in photodynamic therapy of cancer. *Molecules.* 2011;16(5):4140-4164.

Williams AC, Barry BW. Penetration enhancers. *Adv Drug Deliv Rev.* 2012;(64):128-137.

Received for publication on 14th December 2021

Accepted for publication on 05th July 2022